BEILSTEIN JOURNAL OF ORGANIC CHEMISTRY

# $MoO_3$ on zeolites MCM-22, MCM-56 and 2D-MFI as catalysts for 1-octene metathesis

Hynek Balcar*, Martin Kubů, Naděžda Žilková and Mariya Shamzhy

Full Research Paper

Open Access

Address:
J. Heyrovský Institute of Physical Chemistry of the Czech Academy of Sciences, v.v.i., Dolejškova 3, 182 23 Prague 8, Czech Republic

Email:
Hynek Balcar* - hynek.balcar@jh-inst.cas.cz

* Corresponding author

Keywords:
metathesis; molybdenum oxide; 1-octene; thermal spreading; zeolites

*Beilstein J. Org. Chem.* **2018,** *14,* 2931–2939.
doi:10.3762/bjoc.14.272

Received: 30 August 2018
Accepted: 15 November 2018
Published: 27 November 2018

This article is part of the thematic issue "Progress in metathesis chemistry III".

Guest Editors: K. Grela and A. Kajetanowicz



## Abstract

Highly active olefin metathesis catalysts were prepared by thermal spreading $MoO_3$ and/or $MoO_2(acac)_2$ on MWW zeolites (MCM-22, delaminated MCM-56) and on two-dimensional MFI (all in $NH_4^+$ form). The catalysts' activities were tested in the metathesis of neat 1-octene (as an example of a longer chain olefin) at 40 °C. Catalysts with 6 wt % or 5 wt % of Mo were used. The acidic character of the supports had an important effect on both the catalyst activity and selectivity. The catalyst activity increases in the order $6MoO_3$/HZSM-5(25) (Si/Al = 25) << $6MoO_2(acac)_2$/MCM-22(70) < $6MoO_3$/2D-MFI(26) < $6MoO_3$/MCM-56(13) < $6MoO_3$/MCM-22(28) reflecting both the enhancing effect of the supports' acidity and accessibility of the catalytic species on the surface. On the other hand the supports' acidity decreases the selectivity to the main metathesis product C14 due to an acid-catalyzed double bond isomerization (followed by cross metathesis) and oligomerization. $6MoO_3$/2D-MFI(26) with a lower concentration of the acidic centres resulting in catalysts of moderate activity but with the highest selectivity.

## Introduction

Molybdenum oxide on silica, alumina or silica-alumina belongs to the well-known and long-time used metathesis catalysts [1]. Albeit typical ill-defined catalysts they are still popular as relatively cheap catalysts finding industrial applications especially in the treatment of low olefins [2-5]. Their catalytic activity depends on many factors, especially on Mo loading, support acidity, and pre-reaction activations. Surface isolated $MoO_4$ tetrahedra were proved as the main precursors of the catalytic species [6,7], thus the perfect dispersion of $MoO_3$ on the surface is a crucial precondition for a high catalytic activity. The mechanisms of transformation of these precursors to the surface Mo carbenes as real catalytically active species has been suggested [6,7]. The replacement of ordinary silicas for mesoporous molecular sieves SBA-15 or MCM-41 increased the

catalyst activity substantially, which allowed performing the metathesis of long chain olefins under mild reaction conditions [8-10]. The positive effect of these supports on the catalyst activity was ascribed to their high surface areas enhancing the spreading of $MoO_3$ molecules on the surface and large pores increasing the substrates/products transport rate.

Microporous zeolites like HZSM-5 impregnated by ammonium heptamolybdate solutions were used for the metathesis of low olefins (ethylene, propylene, butenes) [11-13]. In the case of bulkier substrates they suffer, however, of micropore size limitations. To overcome these limitations a decrease in crystal size and the application of two-dimensional zeolites can be used [14-17]. Two dimensional 2D-MFI and MWW delaminated zeolite MCM-56, which have been prepared recently [18-21], represent two types of these materials, which exhibit relatively high surface areas and high accessibility of catalytic sites on the surface as well [22]. Therefore, we supported $MoO_3$ and/or $MoO_2(acac)_2$ on (i) 2D-MFI (and ordinary HZSM-5 for comparison) and similarly on (ii) MCM-56 and its 3D analogue MCM-22 (both in $NH_4^+$ form) and examined their activity in the metathesis of neat 1-octene (Scheme 1) under ambient pressure and 40 °C. According to our best knowledge, none of these materials have been tested as supports for $MoO_3$ based catalysts for metathesis of higher alkenes up to now. $MoO_x$ on MCM-22 combined with γ-$Al_2O_3$ was used in cross metathesis of 2-butene and ethylene in a stream (125 °C, 1 MPa) [23]. MCM-22, and MCM-56 were also used as supports for Hoveyda–Grubbs type hybrid catalysts active in metathesis of long-chain unsaturated esters [24].

# Results and Discussion

## Catalyst preparation and characterization

XRD patterns and texture properties (Table 1, Figure 1 A,B,C,D) of prepared MCM-22, MCM-56 and 2D-MFI zeolites proved a high quality of these supports. For catalyst labelling following the mode has been adopted: *x* $MoO_3$/MCM-22(*y*), where *x* = Mo concentration in wt % Mo, *y* = Si/Al molar ratio. After spreading Mo compounds over the support surface areas ($S_{BET}$, $S_{ext}$) as well as void volumes ($V$) decreased. Similar reduction of these quantities has been already observed earlier [9,10,24]. For *x* $MoO_3$/MCM-22(28), XRD patterns of catalysts are similar to those of their parents approximately up to *x* = 6 wt % of Mo (0.9 Mo atoms per $nm^2$). At higher Mo concentrations signals of crystalline $MoO_3$ appeared (marked with * in Figure 1 A,B,D). It suggests 6 wt % of Mo being the optimal Mo loading. On the other hand, *x* $MoO_3$/MCM-22(70) catalyst with *x* = 6 wt % Mo exhibited slight $MoO_3$ signals, when prepared from $MoO_3$ probably due to the lower surface area (especially external one) comparing with MCM-22(28). However, when $MoO_2(acac)_2$ was used as a source of Mo, catalysts with 6 wt % (and lower) content of Mo did not exhibit any $MoO_3$ signals. It is consistent with the previous observation that $MoO_2(acac)_2$ provided better catalyst than $MoO_3$ [9]. XRD patterns of 6$MoO_3$/MCM-56(13) and 6$MoO_3$/2D-MFI(26) indicated also a good $MoO_3$ spreading, contrary to 6$MoO_3$/HZSM-5(25) where $MoO_3$ signals were clearly visible, probably as a result of lower external surface area.

**Table 1:** Texture properties of catalysts and corresponding supports.

| | catalyst | $S_{BET}$ ($m^2$/g) | $S_{ext}$ ($m^2$/g) | $V$ ($cm^3$/g) |
|---|---|---|---|---|
| 1 | MCM-22(28) | 455 | 119 | 0.59 |
| 2 | 6$MoO_3$/MCM-22(28) | 423 | 119 | 0.38 |
| 3 | 6$MoO_2(acac)_2$/MCM-22(28) | 426 | 94 | 0.57 |
| 4 | MCM-22(70) | 421 | 58 | 0.29 |
| 5 | 6$MoO_3$/MCM-22(70) | 180 | 39 | 0.25 |
| 6 | 6$MoO_2(acac)_2$/MCM-22(70) | 355 | 41 | 0.24 |
| 7 | 2D-MFI(26) | 565 | 343 | 0.61 |
| 8 | 6$MoO_3$/2D-MFI(26) | 478 | 221 | 0.57 |
| 9 | MCM-56(13) | 469 | 164 | 0.57 |
| 10 | 6MoO3/MCM-56(13) | 269 | 129 | 0.55 |
| 11 | HZSM-5(25) | 410 | 44 | 0.23 |
| 12 | 6MoO3/HZSM-5(25) | 388 | 38 | 0.23 |

$S_{BET}$ = BET area, $V$ = total void volume ($p/p_0$ = 0.95), $S_{ext}$ = external surface (from *t*-plot).

Contrary to the all-siliceous mesoporous sieves (like SBA-15) which are neutral, zeolites are acidic and their acidity (both Brønsted and Lewis-type) plays an important role for catalysis. The acid site concentrations of zeolitic supports and the corresponding catalysts measured using FTIR spectroscopy of adsorbed pyridine are shown in Table 2, while the relevant IR spectra are shown in Supporting Information File 1 (Figures S1–S5). It is seen that all supports contained both Brønsted and Lewis acid sites of various strength. MCM-22(28) and MCM-56(13) exhibited the highest concentrations of acid sites (both Brønsted and Lewis) in accord with their highest Al concentrations. The acid sites concentrations of MCM-22(70) and 2D-MFI(26) were lower and close to each other. The Brønsted acid site concentration of HZSM-5(25) was as high as that of

$$2\ CH_2{=}CH(CH_2)_5CH_3 \rightleftharpoons CH_2{=}CH_2 + CH_3(CH_2)_5CH{=}CH(CH_2)_5CH_3$$

**Scheme 1:** 1-Octene metathesis reaction.

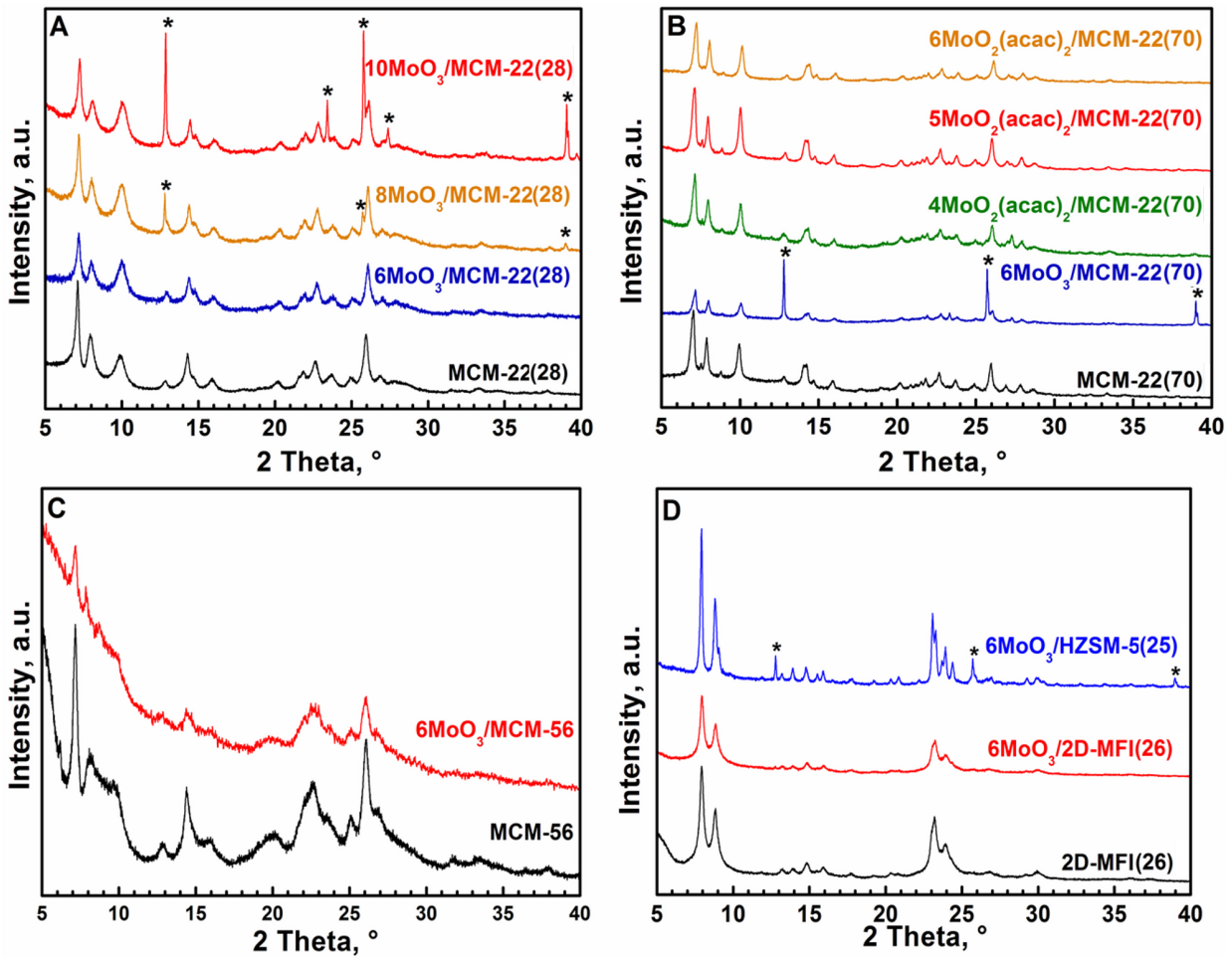


**Figure 1:** A,B,C,D: XRD patterns of parent supports and catalysts used. Asterisk marks $MoO_3$.

**Table 2:** Acid site concentrations in catalysts and corresponding supports.[a]

| sample | $c$(B)[b], mmol/g | | | | $c$(L)[c], mmol/g | | | |
|---|---|---|---|---|---|---|---|---|
| | 150 °C | 250 °C | 350 °C | 450 °C | 150 °C | 250 °C | 350 °C | 450 °C |
| MCM-22(70) | 0.11 | 0.12 | 0.09 | 0.02 | 0.06 | 0.04 | 0.03 | 0.03 |
| $6MoO_3$/MCM-22(70) | 0.02 | 0.01 | – | – | 0.10 | 0.01 | 0.01 | – |
| $6MoO_2(acac)_2$/MCM-22(70) | 0.06 | 0.06 | 0.05 | 0.02 | 0.16 | 0.07 | 0.04 | 0.03 |
| MCM-22(28) | 0.29 | 0.32 | 0.30 | 0.19 | 0.13 | 0.09 | 0.08 | 0.06 |
| $6MoO_3$/MCM-22(28) | 0.07 | 0.09 | 0.07 | 0.04 | 0.31 | 0.10 | 0.03 | 0.01 |
| $6MoO_2(acac)_2$/ MCM-22(28) | 0.09 | 0.07 | 0.05 | 0.02 | 0.23 | 0.08 | 0.03 | 0.01 |
| 2D-MFI(26) | 0.13 | 0.13 | 0.08 | 0.02 | 0.07 | 0.07 | 0.06 | 0.04 |
| $6MoO_3$/2D-MFI(26) | 0.06 | 0.04 | 0.03 | 0.01 | 0.10 | 0.03 | 0.01 | – |
| HZSM-5(25) | 0.29 | 0.28 | 0.22 | 0.07 | 0.04 | 0.03 | 0.02 | 0.02 |
| $6MoO_3$/HZSM-5(25) | 0.14 | 0.12 | 0.09 | 0.03 | 0.17 | 0.07 | 0.04 | 0.04 |
| MCM-56(13) | 0.23 | 0.17 | 0.13 | 0.04 | 0.18 | 0.12 | 0.09 | 0.08 |
| $MoO_3$/MCM-56(13) | 0.04 | 0.03 | 0.01 | – | 0.17 | 0.06 | 0.03 | 0.02 |

[a]Determined by FTIR. [b]Brønsted acid site. [c]Lewis acid site.

MCM-22(28), however, its Lewis acid site concentration was significantly lower. After supporting Mo compounds the concentrations of Brønsted acid sites decreased significantly which may indicate that $MoO_x$ species reacted predominantly with Brønsted acid sites of the supports. It is manifested by intensity decrease of the band in the region 3609–3625 $cm^{-1}$, ascribed to OH vibration in the Si–O(H)–Al acid site (see Supporting Information File 1, Figures S1–S5) [25]. On the other hand, the concentrations of Lewis acid sites in the catalysts was slightly higher compared to the parent supports. It may be explained by the formation of some amount of Mo in a lower oxidation state which has been already described for siliceous supports (MCM-41, SBA-15) [9,26].

## Catalytic activity

### MCM-22-based catalysts

$Na^+$ forms of zeolites turned out to be unsuitable supports for metathesis catalysts. For example, by supporting $MoO_3$ on MCM-22(28) in $Na^+$ form (6 wt % of Mo) we obtained material providing only 0.5% 1-octene conversion in 19 h (1-octene/Mo = 320, $t$ = 40 °C). Therefore, we converted $Na^+$ forms to $NH_4^+$ forms, which were used for supporting Mo compounds by thermal spreading method.

The time development of 1-octene conversion over $6MoO_3$/MCM-22(28) is shown in Figure 2. The GC chromatogram of the final product is shown in Figure S6 (in Supporting Information File 1). It is seen that in addition to the main metathesis product (7-tetradecene), alkenes from C13 to C9 are present in considerable amounts. It is a consequence of the 1-octene double bond isomerization followed by cross metathesis. Moreover, a certain amount of oligomers (mainly dimers) were also observed in the reaction mixtures. Both isomerization and oligomerization are due to the acidic character of the support (vide infra). In addition to the total conversion of 1-octene ($K_{tot}$), the conversion to all metathesis products ($K_{met}$), and the conversion to tetradecene ($K_{C14}$) calculated according to the following equations are plotted in Figure 2.

$$K_{tot} = \frac{(2\Sigma m_i/M_i + 2m_d/M_d + 3m_t/M_t)}{(2\Sigma m_i/M_i + 2m_d/M_d + 3m_t/M_t + m_{C8}/M_{C8})}$$

$$K_{met} = \frac{(2\Sigma m_i/M_i)}{(2\Sigma m_i/M_i + 2m_d/M_d + 3m_t/M_t + m_{C8}/M_{C8})}$$

$$K_{C14} = \frac{(2m_{C14}/M_{C14})}{(2\Sigma m_i/M_i + 2m_d/M_d + 3m_t/M_t + m_{C8}/M_{C8})}$$

where $m_i$ and $M_i$ (i = 9–14) are weight amounts and molecular weights of alkenes from C9 to C14; $m_d$, $m_t$ and $M_d$, $M_t$ are weight amounts and molecular weights of octene dimers and trimers, respectively; $m_{C8}$ is weight amount of octene (all isomers) and $M_{C8}$ is the molecular weight of octene.

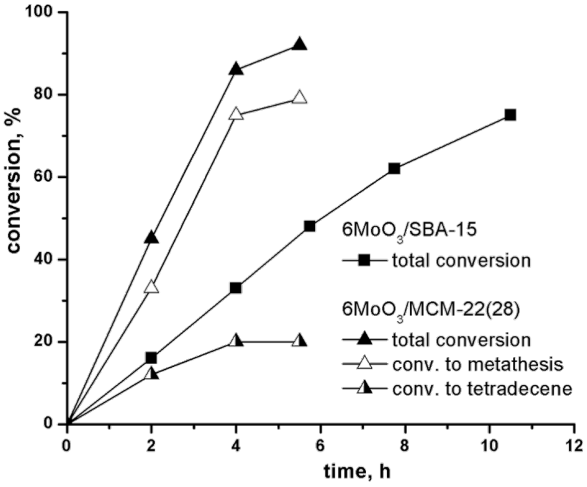


**Figure 2:** Conversion vs time curves for 1-octene metathesis over $6MoO_3$/MCM-22(28) and $6MoO_3$/SBA-15. Neat 1-octene, 1-octene/Mo = 320, $t$ = 40 °C.

For comparison, the conversion curve over $6MoO_3$/SBA-15 is added in Figure 2. $6MoO_3$/SBA-15 was prepared from all-siliceous SBA-15 ($S_{BET}$ = 877$m^2$/g, $V$ = 1.07$cm^3$/g, pore diameter $D$ = 6.4 nm) and it is known as a very active and selective catalyst [9,10]. Under reaction conditions applied the selectivity to tetradecene was about 98% during the whole experiment, and therefore only $K_{tot}$ is plotted in Figure 2 in this case.

Both $K_{tot}$ and $K_{met}$ for $6MoO_3$/MCM-22(28) were significantly higher than the total conversion for $6MoO_3$/SBA-15 (Figure 2). Conversions to oligomers ($K_{ol} = K_{tot} - K_{met}$) were about 12% (at 2 h) and practically did not change in the further course of the reaction. However, the conversions to tetradecene were rather low (maximum conversion about 20% was achieved). Higher catalytic activity of molybdenum oxide on zeolitic support in metathesis may be ascribed to the higher acidity of supports. The enhancing effect of Brønsted acidity on the catalytic activity has been already described [6] and it assumed that most of Mo active species in zeolite-based catalysts are formed by reacting molybdenum oxide with Si-O(H)-Al groups [12,27]. Similarly, Lim et al. showed recently [28], that Brønsted acid sites improve dispersion of molybdenum oxide on the surface. Moreover, for related system based on tungsten oxide in zeolite, it was suggested using high resolution STEM that Brønsted acid sites in proximity to metathesis active sites facilitate olefin adsorption and metallocycle formation [29]. Such mechanism may be effective also for Mo catalysts. The decrease in the selectivity due to isomerization and/or oligomerization seems to be an unavoidable cost for this activity enhancement.

It is known for molybdenum oxide catalysts, that with increasing Mo loading the catalytic activities increase up to maximum value [6,10]. At higher loadings the molybdenum oxide spreading on the surface became imperfect and catalytically inactive bulk $MoO_3$ appears. The effect of increasing Mo loading on catalyst activity for MCM-22(28)-based catalyst is shown in Table 3.

For $8MoO_3$/MCM-22(28) XRD pattern shows a small amount of bulk $MoO_3$ (marked with asterisk in Figure 1A). In accord with this, the conversions fell down in comparison with $6MoO_3$/MCM-22(28), the selectivity, however, slightly increased: the amount of oligomers was reduced and the selectivity to the tetradecene approximately doubled. It suggests that more acid sites were covered by $MoO_x$ species and oligomerization and isomerization ability of catalysts decreased. However, further increase in the Mo loading to 10 wt % in $10MoO_3$/MCM-22(28) led nearly to the lost of catalytic activity, which is explained by deposition of Mo in the catalytically inactive bulk $MoO_3$. Correspondingly, very intensive diffraction lines of the bulk $MoO_3$ appeared in the XRD pattern of $10MoO_3$/MCM-22(28) (see Figure 1A).

To reduce isomerization and oligomerization ability of MCM-22-based catalysts we prepared zeolite with Si/Al = 70 (and therefore with lower acidity – vide supra): MCM-22(70). The results showing the catalytic behavior of the prepared MCM-22(70)-based catalysts $6MoO_2(acac)_2$/MCM-22(70), $5MoO_2(acac)_2$/MCM-22(70), and $4MoO_2(acac)_2$/MCM-22(70) are collected in Table 4.

XRD pattern of $6MoO_3$/MCM-22(70) exhibited some amount of bulk $MoO_3$ (Figure 1B). Evidently on this less acidic support the $MoO_3$ spreading is not perfect, which explains its negligible activity in metathesis reaction. However, using bis(acetylacetonate) complex $MoO_2(acac)_2$ as a source of Mo we obtained $6MoO_2(acac)_2$/MCM-22(70), $5MoO_2(acac)_2$/MCM-22(70), and $4MoO_2(acac)_2$/MCM-22(70) exhibiting no signals of bulk $MoO_3$ in XRD pattern (Figure 1B) and showing a mild metathesis activity. The highest conversion $K_{tot}$ = 35% (after

**Table 3:** The effect of Mo loading on catalyst activity in 1-octene metathesis.[a]

| catalyst | reaction time, h | $K_{tot}$, % | $K_{met}$, % | $K_{ol}$, % | $K_{C14}$, % |
|---|---|---|---|---|---|
| $6MoO_3$/MCM-22(28) | 2 | 45 | 33 | 12 | 12 |
| | 4 | 86 | 75 | 11 | 20 |
| | 6 | 92 | 79 | 13 | 20 |
| $8MoO_3$/MCM-22(28) | 2 | 21 | 15 | 6 | 10 |
| | 4 | 41 | 35 | 6 | 18 |
| | 6.5 | 58 | 51 | 7 | 25 |
| | 22 | 85 | 77 | 8 | 36 |
| $10MoO_3$/MCM-22(28) | 2 | 2.6 | 0.6 | 2 | 0.6 |
| | 4 | 3.4 | 0.7 | 2.7 | 0.7 |
| | 6 | 4 | 1 | 3 | 1 |

[a]50 mg Catalyst, 1.5 mL 1-octene, 40 °C.

**Table 4:** 1-Octene metathesis over MCM-22(70)-based catalysts.[a]

| catalyst | reaction time, h | $K_{tot}$, % | $K_{met}$, % | $K_{ol}$, % | $K_{C14}$, % |
|---|---|---|---|---|---|
| $6MoO_3$/MCM-22(70) | 2 | 2 | – | – | – |
| | 4.5 | 3 | | | |
| | 6 | 2 | | | |
| $6MoO_2(acac)_2$/MCM-22(70) | 2 | 8 | 7.5 | 0.5 | 5 |
| | 4 | 9 | 8 | 1 | 6 |
| | 22 | 11.5 | 10.5 | 1 | 7 |
| $5MoO_2(acac)_2$/MCM-22(70) | 2.3 | 8 | 7 | 1 | 5 |
| | 3.3 | 11 | 10 | 1 | 7 |
| | 20 | 35 | 32 | 3 | 17 |
| $4MoO_2(acac)_2$/MCM-22(70) | 2 | 11 | 11 | 0 | 10 |
| | 4 | 16 | 15 | 1 | 14 |
| | 21 | 16 | 15 | 1 | 14 |

[a]50 mg Catalyst, 1.5 mL 1-octene, 40 °C.

20 h) was achieved over $5MoO_2(acac)_2$/MCM-22(70). Oligomerization activity of all these catalysts was considerably lower in comparison with that of $6MoO_3$/MCM-22(28) ($K_{ol}$ = 1% only). However, the isomerization was not suppressed and conversion to tetradecene $K_{C14}$ was low.

### MCM-56-based catalysts

Conversion curves for the 1-octene metathesis over $6MoO_3$/MCM-56(13) under standard conditions are displayed in Figure 3. In spite of the 2D character of support the conversions over $6MoO_3$/MCM-56(13) were significantly lower in comparison with $6MoO_3$/MCM-22(28): the initial reaction rate (calculated at reaction time = 2 h) being about a half of the initial reaction rate over $6MoO_3$/MCM-22(28). On the other hand the extent of oligomerization was practically the same (for final product the oligomerization selectivity was 14%) and the extent of cross metathesis was even higher (the selectivity to tetradecene was only 15%). The crystals of MCM-22 (see SEM image in Supporting Information File 1, Figure S7) consist of very thin platelets and therefore a great amounts of 12-membered ring cups of MWW structure are on crystal exterior [18]. These cups as we assume host $MoO_x$ species. Although MCM-56(13) as 2D zeolite consists of very thin layers, these layers may be curled and packed, which prevents the access of substrate molecules to the most of 12MR cups (for MCM-56(13) morphology see Supporting Information File 1, Figure S8). This may explain the lower activity of $6MoO_3$/MCM-56(13) compared with $6MoO_3$/MCM-22(28). Similarly, a higher activity of MCM-22 in comparison with MCM-56 has been observed in toluene disproportionation [18] and also for RCM of citronellene over immobilized Ru catalysts the activity of catalyst based on MCM-56 was not higher than that based on MCM-22 [24].

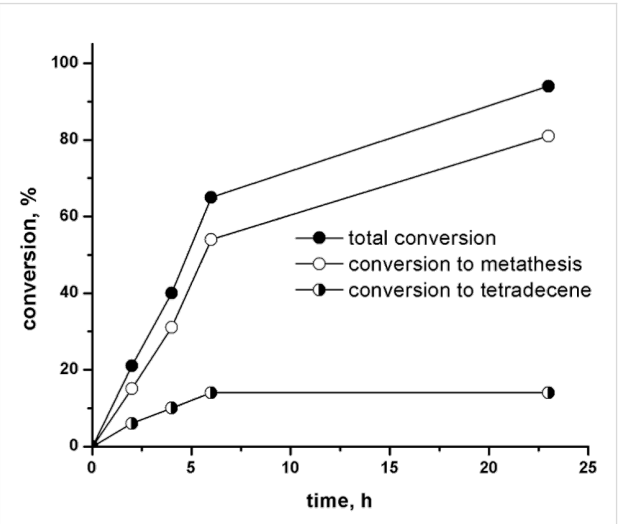


**Figure 3:** Conversion vs time curves for the 1-octene metathesis over $6MoO_3$/MCM-56(13). Neat 1-octene, 1-octene/Mo = 320, $t$ = 40 °C.

### MFI-based catalysts

The comparison of conversion curves for 1-octene over $6MoO_3$/2D-MFI(26) and $6MoO_3$/HZSM-5(25) under standard conditions is given in Figure 4. It is seen that $6MoO_3$/HZSM-5(25) exhibited only negligible activity ($K_{tot} = K_{met}$ = 3% after 20 h) in accord with poor $MoO_3$ spreading (see Figure 1D). Despite the high acidity of the support, a poor accessibility of relevant surface OH groups during the thermal spreading process and a poor accessibility of possible active sites by substrate molecule during metathesis may cause $6MoO_3$/HZSM-5(25) to be practically inactive. On the other hand, over $6MoO_3$/2D-MFI(26) about 90% conversion was achieved for the same reaction time (20 h). The initial reaction rate over $6MoO_3$/2D-MFI(26) was only slightly lower than that over $6MoO_3$/MCM-56(13) and about one half of that over $6MoO_3$/MCM-22(28). Contrary to $6MoO_3$/MCM-22(28) the oligomerization activity of $6MoO_3$/2D-MFI(26) was reduced ($K_{ol}$ was from 1% to 5%) and the selectivity to tetradecene was higher (for final conversions $K_{C14}/K_{met}$ = 0.41 and 0.25 for $6MoO_3$/2D-MFI(28) and $6MoO_3$/MCM-22(28), respectively). Lower acidity of $6MoO_3$/2D-MFI(28) may explain the lower extent of oligomerization and isomerization reactions and increased tetradecene selectivity. Lower acidity may also bring about the reduced activity as compared with $6MoO_3$/MCM-22(28); however, different structures of MCM-22 and MFI do not allow simple comparison.

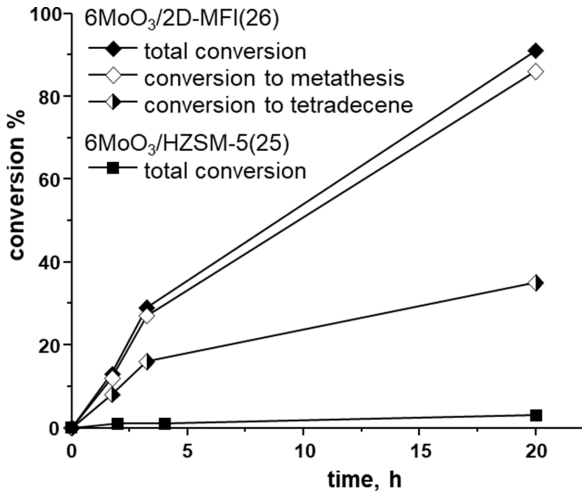


**Figure 4:** Conversion vs time curves for 1-octene metathesis over $6MoO_3$/2D-MFI(26) and 6MoO3/HZSM-5(25). Neat 1-octene, 1-octene/Mo = 320, $t$ = 40 °C.

## The accompanying oligomerization activity

The experiments with Mo-free zeolites (Figure 5a,b) confirmed that the oligomerization activity was connected with the support itself. In these "blank" experiments the reaction conditions, as well as pretreatment mode were the same as for Mo oxide cata-

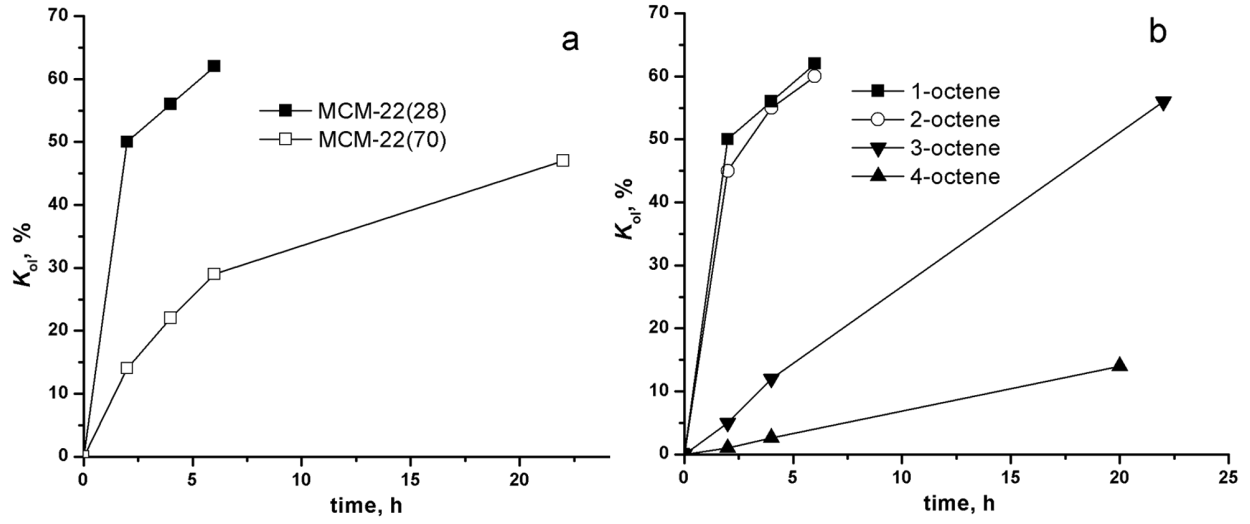


**Figure 5:** Conversion to oligomers for 1-octene over MCM-22(28) and MCM-22(70) (a) and conversion to oligomers for 1-octene, 2-octene, 3-octene, and 4-octene over MCM-22(28) (b). 50 mg Support, 1.5 mL octene, 40 °C.

lysts. No metathesis products were observed, only 1-octene oligomerization and double bond isomerization occurred. Figure 5a shows 1-octene oligomerization over MCM-22(28) and MCM-22(70). Families of dimers and trimers (in weight ratio dimers/trimers approximately 20:1 for the final conversions) were detected, isolation and characterization of individual dimers/trimer was not possible. It was visible from GC, that isomerization of starting 1-octene also occurred, however, the exact quantification was not possible. The oligomerization rate was higher for MCM-22(28) in accord with its higher acidity as compared with MCM-22(70). The extent of oligomerization in these blank experiments is several times higher than that achieved over metathesis catalysts: it may be due to the partial capping of support acid sites with Mo species catalysts and also due the parallel consumption of 1-octene in metathesis.

Figure 5b shows oligomerization of 1-octene, 2-octene (*cis* + *trans*), 3-octene (*trans*), and 4-octene (*trans*) over MCM-22(28). It is seen that the initial reaction rate decreases in the order 1-octene ≈ 2-octene > 3-octene > 4-octene. The low-temperature oligomerization of alkenes over zeolite was studied as concerns industrially important low alkenes oligomerization and lower reactivity of internal alkenes in comparison with 1-alkenes was also recognized [30,31]. The reduced activity of 3- and 4-octenes in oligomerization might explain the fact, that in our metathesis experiments the accompanying oligomerization occurred practically only in the beginning of the reaction. In later stages when most of 1-octene was isomerized to 3- and 4-octenes only little increase in oligomer amounts was observed.

## Conclusion

3D and 2D zeolites of MWW (MCM-22 and MCM-56) and MFI topologies were used for the first time as supports for the preparation of highly active molybdenum oxide metathesis catalysts. The catalysts, prepared by thermal spreading of $MoO_3$ and/or $MoO_2(acac)_2$ on these supports in $NH_4^+$ forms (6 wt % and/or 5 wt % of Mo) were tested in neat 1-octene metathesis under mild conditions (batch reactor, atmospheric pressure, 40 °C).

The catalyst activity (expressed as $K_{tot}$ values at the reaction time = 2 h) decreased in the order $6MoO_3$/MCM-22(28) > $6MoO_3$/MCM-56(13) > $6MoO_3$/2D-MFI(26) > $6MoO_2(acac)_2$/MCM-22(70) >> $6MoO_3$/HZSM-5(25). This activity order reflects two effects enhancing the activity: (i) support acidity and (ii) structure characteristics ensuring good accessibility of active species by substrate molecules. The most active $6MoO_3$/MCM-22(28) exhibited a significantly higher activity than that of a similar catalyst supported on siliceous mesoporous molecular sieve SBA-15.

Due to the catalyst acidity accompanying reactions occurred: (i) 1-octene double bond isomerization followed by cross metathesis and (ii) 1-octene oligomerization (mainly dimerization). The extent of these reactions depends strongly on the support acidity. Highly acidic supports MCM-22(28) and MCM-56(13) delivered a catalyst of rather low selectivity (up to 14% conversion to oligomers, 15–20% conversion to tetradecene at about $K_{tot}$ = 90%). Less acidic supports – MCM-22(70) and 2D-MFI(26) gave rise catalysts of significantly higher selec-

tivity: conversion to oligomers was reduced to 1%, double bond isomerization and cross metathesis proceeded in less extent, so selectivity to tetradecene increased (e.g., for 2D-MFI(26) to 35% at $K_{tot}$ = 90%).

It is seen that for the metathesis of longer chain hydrocarbons like 1-octene, supports ensuring a good access of bulkier substrate to the active centers are necessary. The acidity of the support increases the catalyst activity, however, simultaneously with decrease of the catalyst selectivity. 2D-MFI(26) due to its moderate acidity and 2D character results in catalysts of moderate activity but of the highest selectivity.

With the described catalysts 1-octene was converted into a mixture of higher olefins: in addition to tetradecene as a homometathesis product, olefins of 9–13 C atoms from cross metathesis and C16 dimers were formed in various extent. Therefore, the described catalysts may find application especially if a mixture of higher olefins is desired, for example in the preparation of detergents, lubricants etc.

# Experimental

## Catalyst preparation and characterization

The zeolite supports MCM-22 and MCM-56 were prepared according to [32,33], 2D-MFI was synthesized according to [21]. HZSM-5 (CBV 5524) was purchased from Zeolyst. $Na^+$ forms of zeolites were converted to $NH_4^+$ form by three-fold treatment with 1.0 M $NH_4NO_3$ solution at room temperature for 3 h. The supports were characterized by XRD (Bruker AXS D8 Advance diffractometer with a graphite monochromator and a Vantec-1 position sensitive detector using Cu Kα radiation in Bragg−Brentano geometry) and by $N_2$ adsorption (77 K, Micromeritics GEMINI II 2370 volumetric Surface Area Analyzer). Molybdenum(VI) oxide (Sigma-Aldrich) and bis(acetylacetonato)dioxomolybdenum(VI) (Aldrich) as sources of Mo oxide species were used for catalyst preparation using the thermal spreading method (500 °C, 8 h). SEM images were recorded using a JEOL JSM-5500LV microscope.

The concentrations of Lewis (*c*L) and Brønsted (*c*B) acid sites were determined by FTIR spectroscopy of adsorbed pyridine (Py) using a Nicolet 6700 with a transmission MCT/B detector. The zeolites were pressed into self-supporting wafers with a density of 8.0–12 mg·cm$^{-2}$ and activated in situ at $T$ = 450 °C and $p = 5 \cdot 10^{-5}$ torr for 4 h. Pyridine adsorption was carried out at 150 °C and a partial pressure of 3.5 torr for 20 min followed by desorption for 20 min at 150, 250, 350 or 450 °C. Before adsorption, pyridine was degassed by freeze–pump–thaw cycles. All spectra were recorded with a resolution of 4 cm$^{-1}$ by collecting 128 scans for a single spectrum at room temperature. The spectra were recalculated using a wafer density of 10 mg·cm$^{-2}$. *c*L and *c*B were evaluated from the integral intensities of bands at 1454 cm$^{-1}$ (*c*L) and 1545 cm$^{-1}$ (*c*B) using extinction coefficients, ε(L)=2.22 cm·mmol$^{-1}$ and ε (B)=1.67 cm·mmol$^{-1}$[34].

For elemental analysis ICP OES (iCAP 7000, Thermo Scientific) was used. About 50 mg of the catalyst was digested in a mixture of HF, HCl, and $HNO_3$ (1:2:2). The samples were placed in a Berghof microwave in a closed vessel at $T$ = 140 °C for 35 min. Saturated solution of $H_3BO_3$ was then added for complexation of the excess of HF. After digestion solutions under analysis were collected in 250 mL flasks and diluted with ultra pure water.

## Catalytic experiments

Catalytic experiments were carried out in an argon atmosphere using a vacuum argon line. 1-Octene (Aldrich, 98%) was passed through alumina and stored with Na. The content of water in 1-octene was about 5 ppm. 2-Octene (Alfa-Aesar, 98%), *trans*-3-octene (Alfa-Aesar, 97%) and *trans*-4-octene (Aldrich) were purified in a similar way. In a typical experiment 50 mg of catalyst (6 wt % of Mo) was used. Before reaction catalyst was pretreated in vacuo at 500 °C for 30 min. After cooling to 40 °C, the reactor was filled with Ar and neat 1-octene (1-octene/Mo ratio = 320) was added under stirring. The reaction progress was followed by GC analysis of reaction mixture samples taken at given intervals. Individual compounds were identified by GC/MS. A high-resolution gas chromatograph Agilent 6890 with a DB-5 column (length: 50 m, inner diameter: 320 μm, stationary phase thickness: 1 μm), equipped with a 7683 Automatic Liquid Sampler and a FID detector and GC/MS (ThermoFinnigan, FOCUS DSQ II single Quadrupole) were used. Conversions were calculated from the mass balance.

# Supporting Information

### Supporting Information File 1

IR spectra of catalysts, GC of reaction products, and SEM images of catalysts.
[https://www.beilstein-journals.org/bjoc/content/supplementary/1860-5397-14-272-S1.pdf]

# Acknowledgements

The authors thank J. Přech (J. Heyrovský Institute) for the preparation of MFI support samples, and Valeryia Kasneryk (J. Heyrovský Institute) for the SEM images. Financial support from the Grant Agency of the Czech Republic (project No. 17-01440S) is gratefully acknowledged.

## References


1. Ivin, K. J.; Mol, J. C. Applications of the Olefin Metathesis Reaction. *Olefin Metathesis and Metathesis Polymerization,* 2nd ed.; Academic Press: London, 1997; pp 397–410. doi:10.1016/b978-012377045-5/50018-5
2. Hahn, T.; Bentrup, U.; Armbrüster, M.; Kondratenko, E. V.; Linke, D. *ChemCatChem* **2014,** *6,* 1664–1672. doi:10.1002/cctc.201400040
3. Zhang, D.; Li, X.; Liu, S.; Huang, S.; Zhu, X.; Chen, F.; Xie, S.; Xu, L. *Appl. Catal., A* **2012,** *439-440,* 171–178. doi:10.1016/j.apcata.2012.07.002
4. Hahn, T.; Kondratenko, E. V.; Linke, D. *Chem. Commun.* **2014,** *50,* 9060–9063. doi:10.1039/c4cc01827c
5. Gholampour, N.; Yusubov, M.; Verpoort, F. *Catal. Rev.: Sci. Eng.* **2016,** *58,* 113–156. doi:10.1080/01614940.2015.1100871
6. Lwin, S.; Wachs, I. E. *ACS Catal.* **2014,** *4,* 2505–2520. doi:10.1021/cs500528h
7. Amakawa, K.; Kröhnert, J.; Wrabetz, S.; Frank, B.; Hemmann, F.; Jäger, C.; Schlögl, R.; Trunschke, A. *ChemCatChem* **2015,** *7,* 4059–4065. doi:10.1002/cctc.201500725
8. Balcar, H.; Čejka, J. *Coord. Chem. Rev.* **2013,** *257,* 3107–3124. doi:10.1016/j.ccr.2013.07.026
9. Balcar, H.; Mishra, D.; Marceau, E.; Carrier, X.; Žilková, N.; Bastl, Z. *Appl. Catal., A* **2009,** *359,* 129–135. doi:10.1016/j.apcata.2009.02.037
10. Topka, P.; Balcar, H.; Rathouský, J.; Žilková, N.; Verpoort, F.; Čejka, J. *Microporous Mesoporous Mater.* **2006,** *96,* 44–54. doi:10.1016/j.micromeso.2006.06.016
11. Lin, B.; Zhang, Q.; Wang, Y. *Ind. Eng. Chem. Res.* **2009,** *48,* 10788–10795. doi:10.1021/ie901227p
12. Handzlik, J. *J. Mol. Catal. A: Chem.* **2010,** *316,* 106–111. doi:10.1016/j.molcata.2009.10.007
13. Li, X.; Zhang, W.; Liu, S.; Han, X.; Xu, L.; Bao, X. *J. Mol. Catal. A: Chem.* **2006,** *250,* 94–99. doi:10.1016/j.molcata.2006.01.046
14. Díaz, U.; Corma, A. *Dalton Trans.* **2014,** *43,* 10292–10316. doi:10.1039/c3dt53181c
15. Roth, W. J.; Nachtigall, P.; Morris, R. E.; Čejka, J. *Chem. Rev.* **2014,** *114,* 4807–4837. doi:10.1021/cr400600f
16. Wei, R.; Yang, H.; Scott, J. A.; Aguey-Zinsou, K.-F.; Zhang, D. *Mater. Today Chem.* **2018,** *8,* 1–12. doi:10.1016/j.mtchem.2018.01.002
17. Opanasenko, M. V.; Roth, W. J.; Čejka, J. *Catal. Sci. Technol.* **2016,** *6,* 2467–2484. doi:10.1039/c5cy02079d
18. Juttu, G. G.; Lobo, R. F. *Microporous Mesoporous Mater.* **2000,** *40,* 9–23. doi:10.1016/s1387-1811(00)00233-x
19. Roth, W. J.; Čejka, J.; Millini, R.; Montanari, E.; Gil, B.; Kubu, M. *Chem. Mater.* **2015,** *27,* 4620–4629. doi:10.1021/acs.chemmater.5b01030
20. Leonowicz, M. E.; Lawton, J. A.; Lawton, S. L.; Rubin, M. K. *Science* **1994,** *264,* 1910–1913. doi:10.1126/science.264.5167.1910
21. Choi, M.; Na, K.; Kim, J.; Sakamoto, Y.; Terasaki, O.; Ryoo, R. *Nature* **2009,** *461,* 246–249. doi:10.1038/nature08288
22. Přech, J.; Pizarro, P.; Serrano, D. P.; Čejka, J. *Chem. Soc. Rev.* **2018,** *47,* 8263–8306. doi:10.1039/c8cs00370j
23. Liu, S.; Li, X.; Xin, W.; Xie, S.; Zeng, P.; Zhang, L.; Xu, L. *J. Nat. Gas Chem.* **2010,** *19,* 482–486. doi:10.1016/s1003-9953(09)60095-5
24. Balcar, H.; Žilková, N.; Kubů, M.; Mazur, M.; Bastl, Z.; Čejka, J. *Beilstein J. Org. Chem.* **2015,** *11,* 2087–2096. doi:10.3762/bjoc.11.225
25. Bordiga, S.; Lamberti, C.; Bonino, F.; Travert, A.; Thibault-Starzyk, F. *Chem. Soc. Rev.* **2015,** *44,* 7262–7341. doi:10.1039/c5cs00396b
26. Topka, P. Molybdenum oxide supported on mesoporous molecular sieves – new catalysts for alkene metathesis and alkyne polymerization. Ph.D. Thesis, Charles University, Prague, 2008.
27. Handzlik, J.; Ogonowski, J.; Stoch, J.; Mikołajczyk, M.; Michorczyk, P. *Appl. Catal., A* **2006,** *312,* 213–219. doi:10.1016/j.apcata.2006.07.002
28. Lim, T. H.; Nam, K.; Song, I. K.; Lee, K.-Y.; Kim, D. H. *Appl. Catal., A* **2018,** *552,* 11–20. doi:10.1016/j.apcata.2017.12.021
29. Zhao, P.; Ye, L.; Sun, Z.; Lo, B. T. W.; Woodcock, H.; Huang, C.; Tang, C.; Kirkland, A. I.; Mei, D.; Edman Tsang, S. C. *J. Am. Chem. Soc.* **2018,** *140,* 6661–6667. doi:10.1021/jacs.8b03012
30. Knifton, J. F.; Sanderson, J. R.; Dai, P. E. *Catal. Lett.* **1994,** *28,* 223–230. doi:10.1007/bf00806051
31. O'Connor, C. T.; Kojima, M. *Catal. Today* **1990,** *6,* 329–349. doi:10.1016/0920-5861(90)85008-c
32. Kresge, C. T.; Roth, W. J.; Simmons, K. G.; Vartuli, J. C. Crystalline oxide material. U.S. Patent 5,229,341, June 20, 1993.
33. Fung, A. S.; Lawton, S. L.; Roth, W. J. Synthetic layered MCM-56, its synthesis and use. U. S. Patent 5,362,697, Nov 8, 1994.
34. Emeis, C. A. *J. Catal.* **1993,** *141,* 347–354. doi:10.1006/jcat.1993.1145


## License and Terms